Inorganic Chemistry
Article

Inorg. Chem. **2009**, *48*, 5061–5072 **5061**
DOI: 10.1021/ic8015657

Recognition Preference of Rhodamine-Thiospirolactams for Mercury(II) in Aqueous Solution

Wei Huang,[†] Chunxia Song,[‡] Cheng He,[*,‡] Guojun Lv,[‡] Xiaoyue Hu,[‡] Xiang Zhu,[‡] and Chunying Duan[*,†]

[†]*Coordination Chemistry Institute, State Key Laboratory of Coordination Chemistry, Nanjing University, Nanjing 210093, P.R. China, and* [‡]*State Key Laboratory of Fine Chemicals, Dalian University of Technology, Dalian 116012, P.R. China*

Received August 16, 2008

This work presents the design, syntheses, photophysical properties and Hg^{2+}-binding of the red-emitting rhodamine derivatives **RS1**, **RS2**, and **RS3** with different coordination ability and different spatial effects that derived from rhodamine thiohydrazone chromophores and respective carboxaldehydes (benzaldehyde, pyridine-2-carboxaldehyde, ferrocenecarboxaldehyde). Chemosensors **RS2** and **RS3** afford turn-on fluorescence enhancement and display high brightness in water with the EC_{50} for Hg^{2+} of 0.5 ppb. The fluorescence intensities are nearly proportional to the amount of Hg^{2+} at ppb level, when employing 100 nM probes in water. The fluorescence responses of these two chemosensors are Hg(II) specific, and the probes are selective for Hg(II) over alkali, alkaline earth metals, divalent first-row transition metal ions, and Group 12 congeners Zn(II) and Cd(II), as well as heavy metals Pb(II) and Ag(I). X-ray crystal structure analyses exhibit the thioether derivative of the spirolactone in these compounds. Hg^{II}-specific binding in water would make the opening of the spirolactam ring and consequently causes the appearance of strong absorption at visible range, and the obvious and characteristic color change from colorless to pink. Compared to the thioamides, the improved selectivity for Hg^{2+} is attributed to the poorer coordination affinity of the thioether over other interference metal ions.

Introduction

The development of selective and sensitive imaging tools capable of monitoring heavy- and transition-metal ions has attracted considerable attention because of the wide use of these metal ions and their subsequent impact on the environment and nature.[1−5] The Hg^{2+} ion is considered highly dangerous because both elemental and ionic mercury can be converted into methyl mercury by bacteria in the environment, which subsequently bioaccumulates through the food chain.[6−8] The Environmental Protection Agency (EPA) standard for the maximum allowable level of inorganic Hg^{2+} in drinking water is 2 ppb.[9] An ideal probe should thus display a very low detection limit in water and retain its selectivity toward Hg^{2+}.[10−12] Current techniques for mercury screening, including atomic absorption/emission spectroscopy and inductively coupled plasma mass spectrometry often require expensive and sophisticated instrumentation or sample preparation. Fluorescence detection of Hg^{2+} offers a promising approach for simple and rapid tracking of mercury ion in biological, toxicological and environmental monitoring.[13−19] An important practical challenge in achieving this goal is devising water-soluble fluorescent dyes that can

*To whom correspondence should be addressed. E-mail: cyduan@dlut.edu.cn.

(1) *Fluorescent Chemosensors for Ion and Molecule Recognition*; Czarnik, A. W., Ed.; American Chemical Society: Washington, DC, **1993**; p 1.
(2) de Silva, A. P.; Gunaratne, H. Q. N.; Gunnlaugsson, T.; Huxley, A. J. M.; McCoy, C. P.; Rademacher, J. T.; Rice, T. E. *Chem. Rev.* **1997**, *97*, 1515–1566.
(3) Liu, J.; Lu, Y. *J. Am. Chem. Soc.* **2003**, *125*, 6642–6643.
(4) Peng, X.; Du, J.; Fan, J.; Wang, J.; Wu, Y.; Zhao, J.; Sun, S.; Xu, T. *J. Am. Chem. Soc.* **2007**, *129*, 1500–1501.
(5) Royzen, M.; Dai, Z.; Cannry, J. W. *J. Am. Chem. Soc.* **2005**, *127*, 1612–1613.
(6) Renzoni, A.; Zino, F.; Franchi, E. *Environ. Res.* **1998**, *77*, 68–72.
(7) Boening, D. W. *Chemosphere* **2000**, *40*, 1335–1351.
(8) Harris, H. H.; Pickering, I. J.; George, G. N. *Science* **2003**, *301*, 1203.
(9) Mercury Update: *Impact on Fish Advisories*, EPA Fact Sheet EPA-823-F-01-011; EPA, Office of Water: Washington, DC, **2001**.
(10) Descalzo, A. B.; Martínez-Máñez, R.; Radeglia, R.; Rurack, K.; Sato, J. *J. Am. Chem. Soc.* **2003**, *125*, 3418–3419.
(11) Nolan, E. M.; Lippard, S. J. *J. Am. Chem. Soc.* **2003**, *125*, 14270–14271.
(12) Nolan, E. M.; Lippard, S. J. *Chem. Rev.* **2008**, *108*, 3443–3480.
(13) Yoon, S.; Albers, A. E.; Wong, A. P.; Chang, C. J. *J. Am. Chem. Soc.* **2005**, *127*, 16030–16031.
(14) Ko, S. K.; Yang, Y. K.; Tae, J.; Shin, I. *J. Am. Chem. Soc.* **2006**, *128*, 14150–14155.
(15) Yoon, S.; Miller, E. W.; He, Q.; Do, P. H.; Chang, C. J. *Angew. Chem., Int. Ed.* **2007**, *46*, 6658–6661.
(16) Yang, H.; Zhou, Z.; Huang, K.; Yu, M.; Li, F.; Yi, T.; Huang, C. *Org. Lett.* **2007**, *9*, 4729–4732.
(17) Nolan, E. M.; Lippard, S. J. *J. Am. Chem. Soc.* **2007**, *129*, 5910–5918.
(18) Prodi, L.; Bargossi, C.; Montalti, M.; Zaccheroni, N.; Su, N.; Bradshaw, J. S.; Izatt, R. M.; Savage, P. B. *J. Am. Chem. Soc.* **2000**, *122*, 6769–677.
(19) Liu, J.; Lu, Y. *Angew. Chem., Int. Ed.* **2007**, *46*, 7587–7590.

Published on Web 05/15/2009

Scheme 1. Structures of Rhodamine Hydrazones and Thiohydrazones for Hg^{2+} Recognition

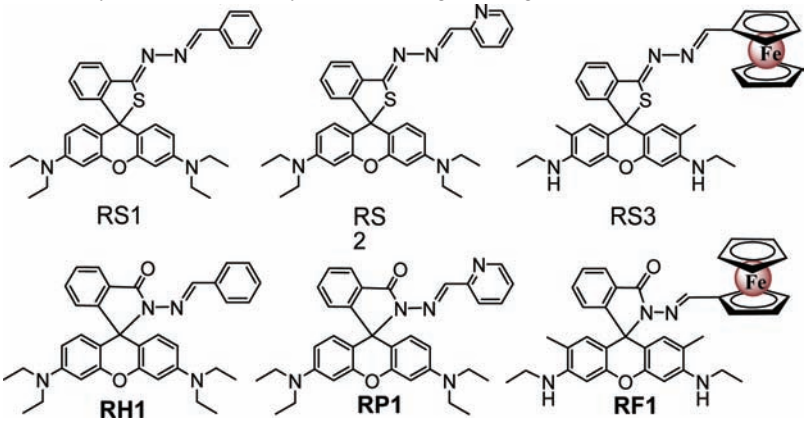

selectively report Hg^{2+} over competing metal ions.[20−25] While several types of small molecule sensors[26,27] and dosimeters,[28−30] materials[31−34] and biomolecules[35−38] have been examined for fluorescent Hg^{2+} detection in aqueous solutions at a parts per billion level, few of them can real-time monitor Hg^{2+} below 1 ppb with the fluorescent responses nearly proportional to the amount of Hg^{2+} in natural water.

Owing to the large molar extinction coefficient (ε) and the high fluorescence quantum yield (Φ), the rhodamine framework is an ideal mode for constructing OFF-ON fluorescent and chromophoric chemosensors because of its particular structural property.[39,40] Very recently, excellent examples of a spirolactam-based chemodosimeter were reported via a Hg^{2+}-induced chemical reaction,[41−43] and a number of rhodamine spirolactams containing a carbohydrazone binding moiety were achieved as highly selective fluorescence chemosensors or multiresponsive chemosensors for detection of Hg^{2+} in aqueous media.[44,45] However, for the selective recognition of such a soft heavy metal ion, a sulfur-based functional group should be considered and introduced.[46,47] Bearing those in mind, we reported here the systematic investigations of rhodamine based chemosensors **RS1**, **RS2**, and **RS3** by combination of a thiospirolacton chromophore and a carbohydrazone block that have different electronic structures, coordination ability, and spatial effects within one molecule (Scheme 1), respectively.

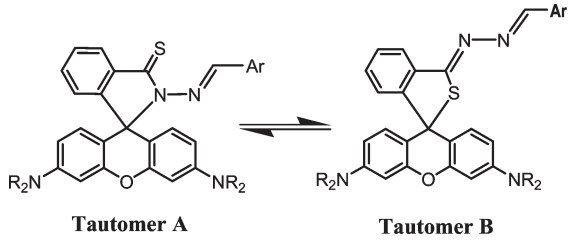

Figure 1. Two possible structures of **RS**s.

Because the C═S double bond is weak, tautomer B would be the major contributor (Figure 1).[48] We thus envision that the metal-binding of the sulfur atom would open the spirolactam ring directly. Meanwhile, the poorer coordination affinity of the thioethers compared to the thioamides suggested the possibly high selectivity for Hg^{2+} over other interference metal ions, especially the thiophilic metal ions, such as Cu^{2+} and Ag^{+}. The potential Hg^{2+}-binding mode and the fluorescence responses mechanism were also systematic investigated.

Experimental Section

Materials. All chemicals used were of reagent grade or obtained from commercial sources and used without further purification except the solvents for physical measurements which were purified by classical methods. The elemental analysis of C, H, and N were performed on a Perkin-Elmer 240 analyzer.

(20) Ko, S. K.; Yang, Y. K.; Tae, J.; Shin, I. *J. Am. Chem. Soc.* **2006**, *128*, 14150–14155.
(21) Zhao, Y.; Zhong, Z. *Org. Lett.* **2006**, *8*, 4715–4717.
(22) Wang, J.; Qian, X. *Org. Lett.* **2006**, *8*, 3721–3724.
(23) Ono, A.; Togashi, H. *Angew. Chem., Int. Ed.* **2004**, *43*, 4300–4302.
(24) Ou, S. J.; Lin, Z. H.; Duan, C. Y.; Zhang, H.; Bai, Z. P. *Chem. Commun.* **2006**, 4392–4394.
(25) Guo, X. F.; Qian, X. H.; Jia, L. H. *J. Am. Chem. Soc.* **2004**, *126*, 2272–2273.
(26) Descalzo, A. B.; Martínez-Máñez, R.; Radeglia, R.; Rurack, K.; Sato, J. *J. Am. Chem. Soc.* **2003**, *125*, 3418–3419.
(27) Métivier, R.; Leray, I.; Valeur, B. *Chem.—Eur. J.* **2004**, *10*, 4480–4490.
(28) Zhang, G.; Zhang, D.; Yin, S.; Yang, X.; Shuai, Z.; Zhu, D. *Chem. Commun.* **2005**, 2161–2163.
(29) Liu, B.; Tian, H. *Chem. Commun.* **2005**, 3156–3158.
(30) Song, K. C.; Kim, J. S.; Park, S. M.; Chung, K. C.; Ahn, S.; Chang, S. K. *Org. Lett.* **2006**, *8*, 3413–3416.
(31) Murkovic, I.; Wolfbeis, O. S. *Sens. Actuators B* **1997**, *39*, 246–251.
(32) Zhang, X.-B.; Guo, C.-C.; Li, Z.-Z.; Shen, G.-L.; Yu, R.-Q. *Anal. Chem.* **2002**, *74*, 821–825.
(33) Safavi, A.; Bagheri, M. *Sens. Actuators B* **2004**, *99*, 608–612.
(34) Huang, C. C.; Yang, Z.; Lee, K. H.; Chang, H. T. *Angew. Chem., Int. Ed.* **2007**, *46*, 6824–6828.
(35) Kim, I. B.; Bunz, U. H. F. *J. Am. Chem. Soc.* **2006**, *128*, 2818–2819.
(36) Zhao, Y.; Zhong, Z. *J. Am. Chem. Soc.* **2006**, *128*, 9988–9989.
(37) Cheng, P.; He, C. *J. Am. Chem. Soc.* **2004**, *126*, 728–729.
(38) Matsushita, M.; Meijler, M. M.; Wirsching, P.; Lerner, R. A.; Janda, K. D. *Org. Lett.* **2005**, *7*, 4943–4946.
(39) Kim, H. N.; Lee, M. H.; Kim, H. J.; Kim, J. S.; Yoon, J. *Chem . Soc. Rev.* **2008**, *37*, 1465–1472.
(40) Lee, M. H.; Wu, J. S.; Lee, J. W.; Jung, J. H.; Kim, J. S. *Org. Lett.* **2007**, *9*, 2501–2504.
(41) Yang, Y. K.; Yook, K. J.; Tae, J. *J. Am. Chem. Soc.* **2005**, *127*, 16760–16761.
(42) Wu, J. S.; Hwang, I. C.; Kim, K.-S.; Kim, J. S. *Org. Lett.* **2007**, *9*, 907–910.
(43) Shi, W.; Ma, H. *Chem. Commun.* **2008**, 1856–1858.
(44) Wu, D. Y.; Huang, W.; Duan, C. Y.; Lin, Z. H.; Meng, Q. J. *Inorg. Chem.* **2007**, *46*, 1538–1540.
(45) Wu, D. Y.; Huang, W.; Lin, Z. H.; Duan, C. Y.; He, C.; Wu, S.; Wang, D. H. *Inorg. Chem.* **2008**, *47*, 7190–7201.
(46) Zheng, H.; Qian, Z. H.; Xu, L.; Yuan, F. F.; Lan, L. D.; Xu, J. G. *Org. Lett.* **2006**, *8*, 859–861.
(47) Zhan, X.-Q.; Qian, Z.-H.; Zheng, Hong.; Su, B.-Y.; Lan, Z.; Xu, J.-G. *Chem. Commun.* **2008**, 1859–1861.
(48) Chae, M.-Y.; Czarnik, A. W. *J. Am. Chem. Soc.* **1992**, *114*, 9704–9705.

Scheme 2. Synthetic Procedure of Chemosensors **RS1**, **RS2**, and **RS3**

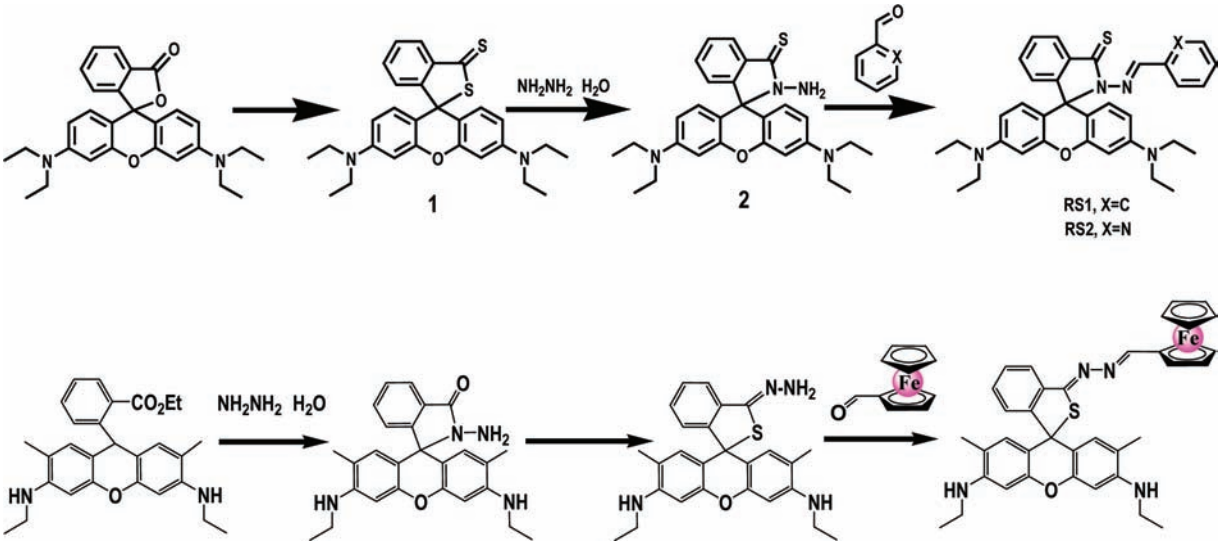

API mass spectra were recorded on HP1100LC/MSD spectrometer. ESI mass spectra were carried out on a HPLC-Q-Tof MS spectrometer using methanol as mobile phase. ^{1}H NMR and ^{13}C NMR spectra were measured on a Varian INOVA 400 M spectrometer at room temperature (Scheme 2).

RS1. Thiooxorhodamine B hydrazide was synthesized according to the literature procedure.[46] Thiooxorhodamine B hydrazide (1.28 mmol, 0.61 g) and benzylaldehyde (1.50 mmol, 0.17 g) were mixed in 30 mL of boiling methanol with addition of 3 drops of acetic acid. After 2 h of refluxing, white precipitates obtained were filtered off, washed with methanol/ether (1:1) and dried under vacuum. Yield: 0.50 g, 70.3%. Anal. Calcd for $C_{35}H_{36}N_4OS$: H, 6.47; C, 74.97; N, 9.99. Found: H, 6.41; C, 74.41; N, 9.60. ^{1}H NMR ($CDCl_3$) δ(ppm): 8.49 (1 H, s, *CH*=*N*), 8.10 (1 H, t, rh-*H*, J = 5.2 Hz), 7.66 (2H, d, ph-*H*, J = 9.2 Hz), 7.39 (2H, t, rh-*H*, J = 4.0 Hz), 7.11 (1H, br, rh-*H*) 6.80(2 H, d, rh-*H*, J = 8.8 Hz), 6.57(2 H, d, rh-*H*, J = 8.8 Hz), 6.31(2H, s, rh-*H*), 6.28 (3H, br, ph-*H*), 3.32 (8 H, q, *N*-CH_2 , J = 6.8 Hz) 1.15 (12 H, t, -CH_3, J = 8.2 Hz). MS: m/z 561.3 for $[RS1 + H]^+$.

RS2. Thiooxorhodamine B hydrazide (1.28 mmol, 0.61 g) and 2-pyridinecarbaldehyde (1.50 mmol, 0.17 g) were mixed in boiling methanol with three drops of acetic acid. After 2 h of stirring, white precipitates obtained were filtered off, washed with methanol/ether (1:1), and dried under vacuum. Yield: 0.42 g, 57.2%. Anal. Calcd for $C_{34}H_{35}N_5OS$: H, 6.28; C, 72.70; N, 12.47. Found: H, 6.34; C, 71.89; N, 12.19. ^{1}H NMR (CD_3Cl) δ(ppm): 8.58 (1H, d, py-*H* J = 7.2 Hz), 8.45 (1 H, s, *CH*=*N*), 8.02 (1 H, d, rh-*H*, J = 7.2 Hz), 7.86 (1 H, d, py-*H*, J = 7.2 Hz), 7.71 (1 H, t, py-*H*, J = 7.2 Hz), 7.68(1 H, t, py-*H*, J = 7.2 Hz), 7.40 (2H, m, rh-*H*), 7.15 (1 H, m, rh-*H*), 6.58 (2 H, d, rh-*H*, J = 12.0 Hz), 6.44 (2 H, d, rh-*H*, J = 12.0 Hz), 6.24 (2 H, s, rh-*H*), 3.13 (8 H, t, *N*-CH_2 J = 12.0 Hz) 1.21 (12 H, t, -CH_3 J = 13.6 Hz); MS: m/z 562.3 for $[RS2 + H]^+$.

RS3. Rhodamine-6G hydrazide was prepared according to the literature method.[49] Rhodamine-6G hydrazide (5.0 mmol, 2.14 g) and Lawesson's Reagent (6.0 mmol, 2.42 g) were dissolved in dry benzene, and the reaction mixture were refluxed for 24 h under N_2 atmosphere. After removal of benzene, the residue was stirred with KOH concentrated for 24 h, and then extracted by CH_2Cl_2. After removal of CH_2Cl_2, the residue was purified by flash chromatography through Al_2O_3 column with CH_2Cl_2 as fluent to afford thiooxo-rhodamine-6G hydrazone (0.60 g, yield: 26.9%). Thiooxorhodamine 6G hydrozone (1.0 mmol, 0.44 g) and ferrocenecarboxaldehyde (1.0 mmol, 0.21 g) were mixed in 20 mL of toluene and 60 mL of methanol with *p*-toluene sulfonic acid (0.1 mmol, 0.019 g). The reaction mixture was refluxed for 20 h under N_2 atmosphere. After cooling to the room temperature, the solvent was evaporated in vacuum. Then the resulting solid was purified by column chromatography (ether: *n*-hexane = 1: 2) to give pink solid. Yield: 0.51 g, 79.6%. Anal. Calcd for $C_{37}H_{36}N_4SOFe$: H, 5.66; C, 69.37; N, 8.75; Found: H, 5.75; C, 68.83; N, 8.66. ^{1}H NMR ($CDCl_3$-d_6) δ(ppm): H 8.04 (1 H, s, *CH*=*N*), 7.88 (1 H, d, rh-*H*, J = 7.2 Hz), 7.57 (1 H, t, rh-*H*, J = 12.8 Hz), 7.52 (1 H, t, rh-*H*, J = 12.8 Hz), 6.98 (1 H, d, rh-*H*, J = 6.4 Hz), 6.37 (2 H, s, rh-*H*), 6.23 (2 H, s, rh-*H*), 4.94 (2H, s, -*NH*), 4.36 (2H, br, Cp-*H*), 4.32 (2 H, br, Cp-*H*), 3.83 (5 H, s, Cp-*H*), 3.16 (4 H, m, -CH_2, J = 7.2 Hz), 1.85 (6 H, s, -CH_3), 1.17 (6 H, t, -CH_3, J = 7.2 Hz). MS: m/z 641.0 for $[RS3 + H]^+$.

Crystallography. Crystallographic data of three compounds were collected on a Bruker APEX CCD diffractometer with graphite-monochromated Mo Kα (λ = 0.71073 Å) using the SMART and SAINT programs.[50] The structures were solved by direct methods and refined on F^2 by full-matrix least-squares methods with SHELXTL version 5.1.[51] Non-hydrogen atoms were refined anisotropically. Hydrogen atoms were fixed geometrically at calculated distances and allowed to ride on the parent non-hydrogen atoms with the isotropic displacement being fixed at 1.2 and 1.5 times of the aromatic and methyl carbon atoms the attached, respectively. For compound **RS2**, two of the ethyl groups were disordered into two parts with the site occupancy factors of the atoms being refined by free variable, respectively. The crystal data of the three compounds were listed in Table 1.

General Spectroscopic Methods. Solution fluorescence titration spectra and selectivity experiments were checked with FS 920 luminescence spectrometer. Stock solution (2×10^{-2} M) of the aqueous perchlorate salts of K^+, Na^+, Ca^{2+}, Mg^{2+}, Fe^{2+}, Co^{2+}, Ni^{2+}, Cu^{2+}, Mn^{2+}, Zn^{2+}, Cd^{2+}, Ag^+, Pb^{2+}, and Hg^{2+} were prepared. High concentration of the stock solutions **RS1**, **RS2** and **RS3** (1.0×10^{-3} M) were prepared in *N*,*N*′-dimethylformamide (DMF). Before spectroscopic measurements, the solution was freshly prepared by diluting the high concentration stock solution to the corresponding solution. For all the titration experiments, spectra were recorded 4 min after

(49) Yang, X.-F.; Guo, X.-Q.; Zhao, Y.-B. *Talanta*. **2002**, *57*, 883–890.

(50) Sheldrick, G. M. *SHELXTL V5.1, Software Reference Manual*; Bruker, AXS, Inc.: Madison, WI, **1997**.

(51) *Regulatory Impact Analysis of the Clean Air Mercury Rule*, EPA-452/R-05-003; U.S. EPA: Research Triangle Park, NC, **2005**.

Table 1. Crystal Data for **RS1**, **RS2**, and **RS3**

compound	**RS1**	**RS2**	**RS3**
molecular formula	$C_{35}H_{36}N_4OS$	$C_{34}H_{35}N_5OS$	$C_{37}H_{36}FeN_4OS$
M_r	560.74	561.73	640.61
crystal system	monoclinic	monoclinic	monoclinic
space group	$P2_1/c$	$P2_1/n$	$P2_1/n$
a/Å	15.786(2)	16.054(2)	8.612(9)
b/Å	12.229(1)	12.228 (1)	22.42(2)
c/Å	17.537(2)	17.190 (2)	21.65(2)
β/deg	115.876(6)	115.556(6)	93.40(2)
V/Å^3	3045.9(6)	3044.6(5)	4172(7)
Z	4	4	4
T/K	298(2)	298(2)	298(2)
D_{calcd} /Mg m^{-3}	1.223	1.225	1.020
μ/mm^{-1}	0.140	0.141	0.439
F(000)	1192	1192	1344
no. refs measured	15771	24319	20322
no. unique refs (R_{int})	5373(0.0372)	5323(0.0747)	7257(0.1072)
no. observed. refs with $I \geq 2\sigma(I)$	3410	2669	2145
R_1[a]	0.0512	0.0487	0.0960
wR_2[a]	0.1460	0.1023	0.2201
goodness of fit	1.069	1.018	1.013

[a] $R_1 = \sum||F_o| - |F_c||/\sum|F_o|$. $wR_2 = [\sum w(F_o^2 - F_c^2)^2/\sum w(F_o^2)^2]^{1/2}$.

adding Hg^{2+} to ensure the reactions come to equilibrium completely. Fluorescence quantum yield (Φ) was determined using optically matching solutions of Rhodamine-6G (Φ_f = 0.94 in ethanol) as standard at an excitation wavelength of 500 nm and the quantum yield is calculated using the equation

$$\Phi_{unk} = \Phi_{std}\frac{(I_{unk}/A_{unk})}{(I_{std}/A_{std})}\left(\frac{\eta_{unk}}{\eta_{std}}\right)^2 \quad (1)$$

where Φ_{unk} and Φ_{std} are the radiative quantum yields of the sample and standard, I_{unk} and I_{std} are the integrated emission intensities of the corrected spectra for the sample and standard, A_{unk} and A_{std} are the absorbances of the sample and standard at the excitation wavelength, and η_{unk} and η_{std} are the indices of refraction of the sample and standard solutions, respectively. Excitation and emission slit widths were modified to adjust the luminescent intensity in a suitable range. All the spectroscopic measurements were performed at least in triplicate and averaged.

Results and Discussions

Structural and Spectroscopic Properties of RS1. Rhodamine spirolactam has been employed to design chemosensors for selective recognition of transition and heavy metal ions, based on the protocol of metal coordination inducing spiro-ring-opening of a sensing molecule.[52−55] As it is well-known, rhodamine derivatives with spirolactam structure are nonfluorescent, whereas ring-opening of the spirolactam gives rise to a strong fluorescence. The longer emission wavelength (over 550 nm) is often preferred to serve as a reporting group for the analyte to avoid the influence of background fluorescence (below 500 nm).[15] We have shown that the carboxyhydrazone moiety might be a proper binding site when incorporated into rhodamine fluorophore.[44,45] The binding event often involves both the carbonyl O and the imino nitrogen atom, forming a stable 5-membered chelating cycle that requires the opening of the spiro ring to establish the delocalized xanthene moiety. Since Hg^{2+} is a soft heavy metal ion, the replacement of the O atom by the S atom has the potential to enhance the sensitivity of the resulting chemosensors toward Hg^{2+}.[43,46,47] On the other hand, several small molecule Hg^{2+} detectors having sulfur-containing macrocycles,[56−59] thioether,[60−62] or thiourea groups[63−65] in the metal-binding units have been reported to exhibit good selectivity for Hg(II). In this regard, a simple receptor of **RS1** was designed and synthesized from rhodamine-thiolactam hydrazide and benzaldehyde.

As shown in Figure 2, X-ray crystallography structural investigation reveals a thiospirocyclic structure with the C_4S spiro ring in solid state with the torsion angle of C(8)−N(1)−N(2)−C(9) of 13°. The C(8)−S(1) distance of 1.742(3) Å and the C(8)═N(1) of 1.287(3) Å demonstrate the existence of a C−S single bond and a C═N double bond in the thiolactam structure. The special structure inhibits the typical emission of Rhodamine B within a relatively wide pH range, such that the emission of **RS1** would be triggered and turned on when it is bound to the target thiophilic cations.

Free **RS1**, as expected, exhibits very weak fluorescence (excited at 510 nm) in DMF/H_2O (1:1, v/v) solution. Upon the addition of Hg^{2+}, the emission band at about

(52) Kwon, J. Y.; Jang, Y. J.; Lee, Y. J.; Kim, K. M.; Seo, M. S.; Nam, W.; Yoon, J. *J. Am. Chem. Soc.* **2005**, *127*, 10107–10111.
(53) Xiang, Y.; Tong, A. *Org. Lett.* **2006**, *8*, 1549–1552.
(54) Xiang, Y.; Tong, A.; Jin, P.; Ju, Y. *Org. Lett.* **2006**, *8*, 2863–2866.
(55) Mao, J.; Wang, L.; Dou, W.; Tang, X.; Yan, Y.; Liu, W. *Org. Lett.* **2007**, *9*, 4567–4570.
(56) Rurack, K.; Kollmannsberger, M.; Resch-Genger, U.; Daub, J. *J. Am. Chem. Soc.* **2000**, *122*, 968–969.
(57) Ros-Lis, J. V.; Martinez-Manez, R.; Rurack, K.; Sancenon, F.; Soto, J.; Spieles, M. *Inorg. Chem.* **2004**, *43*, 5183–5185.
(58) Jimenez, D.; Martinez-Manez, R.; Sancenon, F.; Soto, J. *Tetrahedron Lett.* **2004**, *45*, 1257–1259.
(59) Yuan, M. J.; Li, Y. L.; Li, J.; Li, C. H.; Lin, X. F.; Lv, J.; Xu, J. L.; Liu, H. B.; Wang, S.; Zhu, D. B. *Org. Lett.* **2007**, *9*, 2313–2316.
(60) Zhao, Q.; Cao, T.; Li, F.; Li, X.; Jing, H.; Yi, T.; Huang, C. *Organometallics* **2007**, *26*, 2077–2081.
(61) Ros-Lis, J. V.; Marcos, M. D.; Martínez−Máñez, R.; Rurack, K.; Soto, J. *Angew. Chem., Int. Ed.* **2005**, *44*, 4405–4407.
(62) Nolan, E. M.; Racine, M. E.; Lippard, S. J. *Inorg. Chem.* **2006**, *45*, 2742–2749.
(63) Hennrich, G.; Walther, W.; Resch-Genger, U.; Sonnenschein, H. *Inorg. Chem.* **2001**, *40*, 641–644.
(64) Lee, M. H.; Cho, B. K.; Yoon, J. Y.; Kin, J. K. *Org. Lett.* **2007**, *9*, 4515–4518.
(65) Zhao, Y.; Lin, Z.; He, C.; Wu, H.; Duan, C. *Inorg. Chem.* **2006**, *45*, 10013–10015.

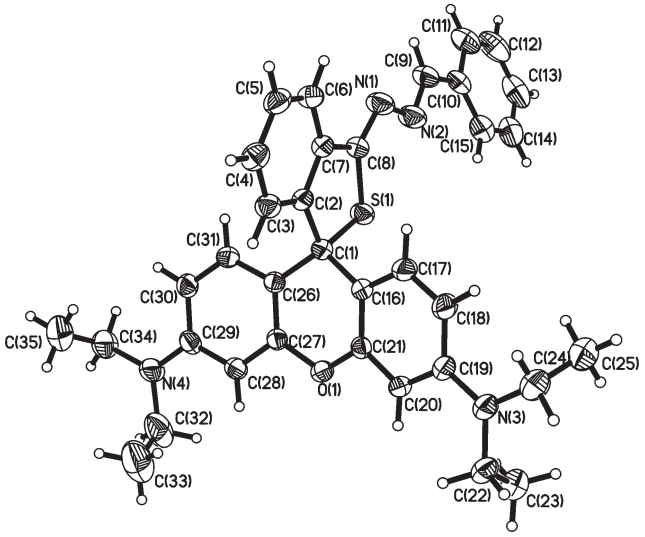

Figure 2. Molecular structure of **RS1** showing the thiospirolactam tautomer. Selected Bond (Å) distances and angles (deg): C(8)−S(1) 1.742(3), C(1)−S(1) 1.895(2), C(8)−N(1) 1.287(3), N(1)−N(2) 1.404(3), N(2)−C(9) 1.267(3); C(8)−S(1)−C(1) 94.2(1), S(1)−C(8)−N(1) 126.5(2), C(8)−N(1)−N(2) 111.3(2), N(1)−N(2)−C(9) 113.7(2), N(2)−C(9)−C(10) 121.7(3).

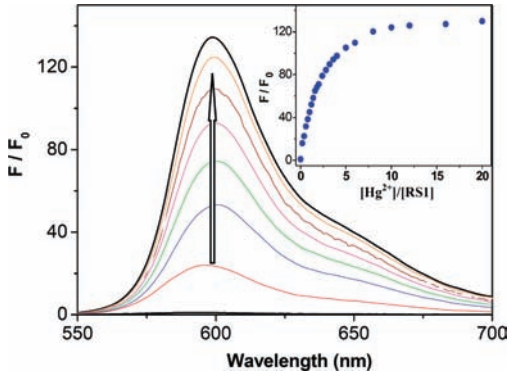

Figure 3. Fluorescence response of **RS1** (10 μM) upon addition of Hg^{2+} (0 to 0.2 mM) in a DMF/H_2O (1:1, v/v) solution (0.1 M KNO_3); the inset picture shows the fluorescence titration profile around 585 nm at the excitation wavelength of 510 nm. Spectra were recorded 4 min after adding Hg^{2+} to ensure the solutions come to quilibrium.

585 nm appears and develops (Figure 3), such an emission band is assigned to the delocalized xanthene tautomer of the rhodamine group.[57] The titration curve shows a steady and smooth increase until a plateau is reached with the quantum yield $\Phi = 0.22$ at the plateau (Figure 3). The pH−control emission measurements reveal that **RS1** can respond to Hg^{2+} in the pH range from 5.5 to 12.0 with the fluorescent intensity varied less than 10%, while the luminescence of the free **RS1** can be negligible. It can be seen that **RS1** facilitates quantification of the concentration of Hg^{2+} in aqueous solution in a wide pH range. When the pH value is lower than 5.0, the fluorescence enhancement occurs also upon the coordination of Hg^{2+}, but the luminescence intensity of the free **RS1** increases slowly with the decreasing pH values.

The fluorescence enhancement effects of various metal ions on **RS1** in DMF/H_2O (1:1, v/v) solution were also investigated (excitation at 510 nm). As illustrated in Figure 4, no significant spectral changes of **RS1** were observed in the presence of alkali-, alkaline-earth metals, such as Na^+, K^+, Mg^{2+}, Ca^{2+} (1.25 mM) and the first-row transition metals Mn^{2+}, Fe^{2+}, Co^{2+}, Ni^{2+}, and Cu^{2+} (0.50 mM), respectively. Even the presence of 0.50 mM of Zn^{2+}, Cd^{2+} as well as Pb^{2+} and Ag^+ could not bring any obvious fluorescence change. The competition experiments revealed that the Hg^{2+}-induced luminescence enhancement was unaffected in the presence of milli-molar (1.25 mM) environmentally relevant alkali-, alkaline-earth metals. In addition, the first-row transition metal ions including Mn^{2+}, Fe^{2+}, Co^{2+}, Ni^{2+}, and Cu^{2+}, as well as Pb^{2+} and Ag^+ (0.50 mM), did not interfere with the Hg^{2+}−induced fluorescence enhancement (the concentration of Hg^{2+} is 0.10 mM), confirming the remarkable selectivity of the probe **RS1** (10 μM) for Hg^{2+}.

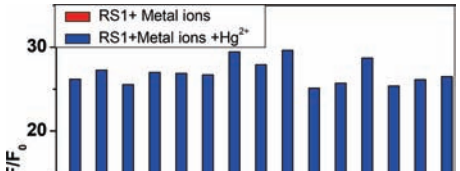

Figure 4. Fluorescence responses of **RS1** to various cations in a DMF/H_2O (1:1, v/v) solution ([**RS1**] = 10 μM; λ_{ex} = 510 nm). The red bars represent the emission intensities of **RF1** in the presence of 1.25 mM of Na^+, K^+, Ca^{2+}, and Mg^{2+} and 0.5 mM of the other cations of interest, respectively. The blue bars represent the change of the emission that occurs upon the subsequent addition of 0.1 mM of Hg^{2+} to the above solution. Spectra were recorded 4 min after mixing the different target ions.

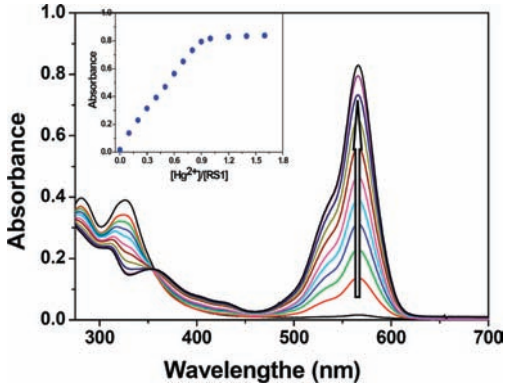

Figure 5. Absorption spectra of **RS1** (50 μM), upon addition of increasing amount of Hg^{2+} in DMF/H_2O (1:1, v/v) solution. The inset shows the titration profile evaluated from the absorption at 585 nm. Spectra were recorded 4 min after adding Hg^{2+}.

The absorption spectra of free **RS1** (50 μM) in DMF/H_2O (1:1, v/v) solution exhibited very weak absorbance from 450 to 700 nm. Upon the addition of Hg^{2+}, the peak around 565 nm was significantly enhanced up to log ε = 4.22, suggesting the formation of the ring-opened tautomer of **RS1** upon Hg^{2+} binding (Figure 5). In this case, the titration solution exhibited an obvious and characteristic color change from colorless to pink. The improved Benesi−Hildebrand analysis of the titration profile[66,67]

(66) Kuntz, I. D.; Gasparro, F. P.; Johnston, M. D.; Taylor, R. P. *J. Am. Chem. Soc.* **1968**, *90*, 4778–4781.
(67) Lin, Z.-H.; Xie, L.-X.; Zhao, Y.-G.; Duan, C.-Y.; Qu, J.-P. *Org. Biomol. Chem.* **2007**, *5*, 3535–3538; supporting information.

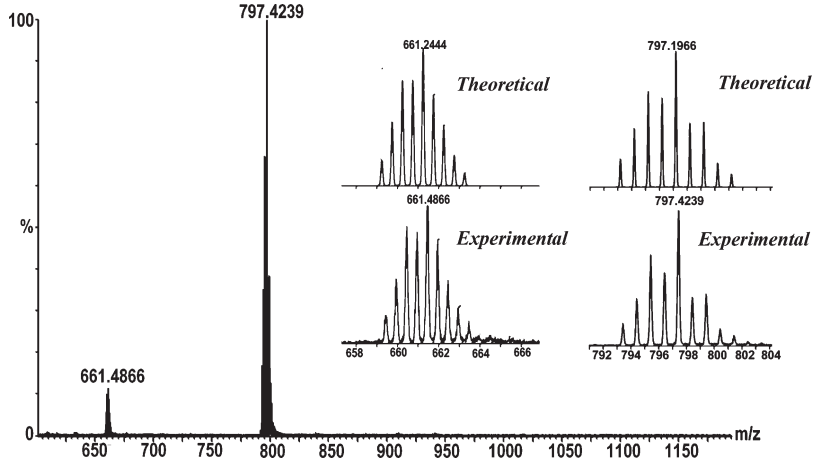

Figure 6. ESI-MS of the titration solution of **RS1** (50 μM) upon the addition of Hg^{2+} (40 μM). The inset exhibits the calculated and observed isotopic patterns for the $[Hg(\mathbf{RS1})_2]^{2+}$ (left) and $[Hg(\mathbf{RS1})(OH)(H_2O)]^{+}$ (right) cations, respectively.

Scheme 3. Proposed Possible Binding Mode of **RS1** with Hg^{2+} [a]

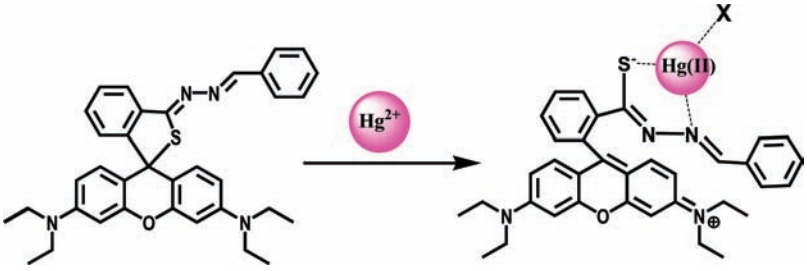

[a] **X** is coordinating anion or solvent.

based on 1:1 stoichiometry for the **RS1**-Hg^{2+} complexation species gives an association constant (K_a) being calculated as 1.82 ($\pm$0.04) $\times$ 10^5 M^{-1}.

ESI-MS of the Hg/**RS1** solution (Figure 6) shows an intense peak with m/z = 797.45, which could be assigned to the Hg^{2+}-binding complexation species [**RS1**-Hg-$(H_2O)(OH)]^+$ (m/z_{calcd} = 797.20), in referring to the exact comparison of the intense peak with the simulation on the basis of natural isotopic abundances. The binding event was proposed to involve both the thioether S and the imino N atom, forming a stable 5-membered cyclic complex that required the opening of the spiro ring to establish the delocalized xanthene moiety. The other coordination sites of Hg^{2+} might be completed by solvents and/or the counter-anions (Scheme 3). The presence of a weak peak at m/z about 661.49 was assigned to [Hg-$(\mathbf{RS1})_2]^{2+}$ complexation species (m/z calcd = 661.24), indicating the presence of trace amount of $[(\mathbf{RS1})_2$-$Hg]^{2+}$ species in the solution.

With further investigations, using a high concentration (i.e., millimolar level) of other transition-metal ions, such as Mn^{2+}, Fe^{2+}, Co^{2+}, Ni^{2+}, Zn^{2+}, and Cd^{2+}, neither a color change nor a fluorescent enhancement was observed (Figure 7). It was suggested that **RS1** did not bind these metal ions simply, though the parent metal-binding functionality thiobenzoylhydrazone was known to bind not only Hg(II) but also the metal ions mentioned above.[68] The addition of Cu^{2+} or Ag^{+} into the solution

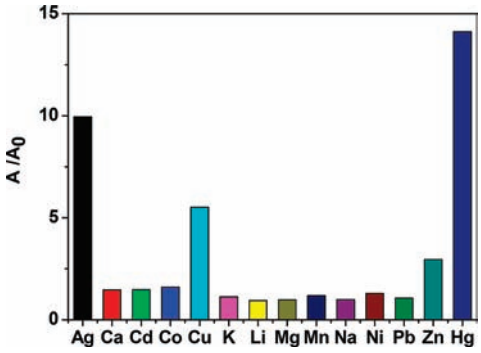

Figure 7. Absorbances at 585 nm of **RS1** (50 μM) in a DMF/H_2O (1:1, v/v) solution in the presence of 5 equiv of different metal ions.

of probe **RS1**, under the same conditions, can induce the small but significant enhancement of the absorbance at about 565 nm. The titration curves exhibit the 1:1 metal/ligand stoichiometry with the binding constant (log K_{ass}) being calculated as 4.28 and 4.45 for Cu^{2+} and Ag^{+}, respectively. However, no significant emission variations could be observed even when the concentration of added Cu^{2+} or Ag^{+} was up to the millimolar level in the fluorescence titration. The excessive Cu^{2+} or Ag^{+} will not compromise the Hg-induced fluorescence. Obviously, the remarkable selectivity for fluorescent detection of Hg^{2+} can be available even in the presence of a high concentration of coexisting metal ions.

Structural and Spectroscopic Properties of RS2. Given that the replacement of pyridine moiety to benzene group in the spirolactam congener can enhance the affinity for

(68) Shen, Y.; Zhang, Y.; Li, Y.; Tao, X.; Wang, Y. *Inorg. Chim. Acta* **2007**, *360*, 1628–1632.

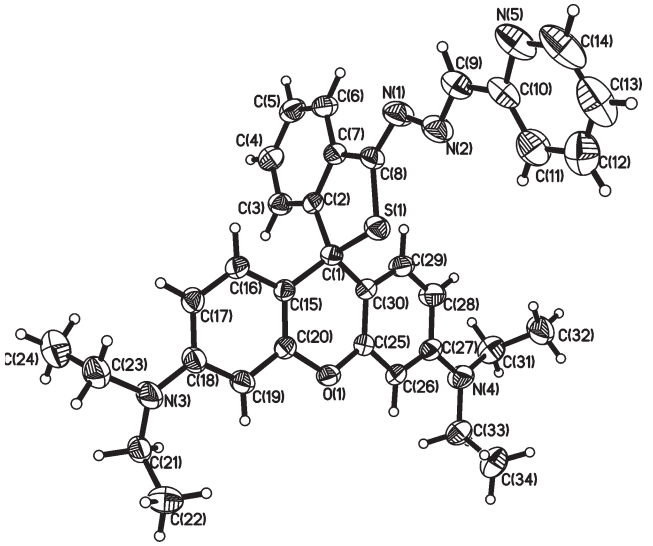

Figure 8. Molecular structure of **RS2** showing the thiospirolactam tautomer. Disordered parts were omitted for clarity. Selected Bond (Å) distances and angles (deg): C(8)−S(1) 1.741(2), C(1)−S(1) 1.889(2), C(8)−N(1) 1.293(3), N(1)−N(2) 1.407(3), N(2)−C(9) 1.268(3); C(8)−S(1)−C(1) 93.9(2), S(1)−C(8)−N(1) 126.2(2), C(8)−N(1)−N(2) 111.1(2), N(1)−N-(2)−C(9) 114.0(2), N(2)−C(9)−C(10) 120.6(3).

Hg^{2+} significantly,[44] we anticipated that the incorporation of pyridine group as part of the metal-binding unit into the thiospirolactam derivative would improve the sensitivity directly. Compound **RS2** was readily synthesized from Rhodamine B thiohydrazone by a one-step reaction. As shown in Figure 8, X-ray crystallography structural investigation reveals the existence of thiospirocyclic structures with the C_4S spiro-ring in solid state. The C(8)−S(1) distance of 1.741(2) Å and the C(8)═N(1) of 1.293(3) Å indicate the existence of a C−S single bond and a C═N double bond of the thiolactam structure. And the prevalence of the thioether tautomer in solution is consistent with detection of a single species by ^{1}H NMR.

The presence of pyridine compared to that of the benzene ring would be favorable to improving solubility. As a result, the chemosensor **RS2** can be used in aqueous solution without additional co-solvent, except the introduction of 0.5% (v/v) of DMF from the stock solution. Free **RS2** exhibited very weak luminescence in aqueous solution when it was excited at 510 nm. Upon the addition of Hg^{2+}, an emission band with the maximum emission wavelength at 585 nm which could be ascribed to the delocalized xanthene moiety of the rhodamine group, appeared and developed, indicating that **RS2** could work as an efficient chemosensor for Hg^{2+} detection in water. The fluorescent titration profile of **RS2** with Hg^{2+} showed a steady and smooth increase until a plateau was reached with a quantum yield of 0.42 (Figure 9), demonstrating that the detection of Hg^{2+} was at the parts per billion level when it was employed at 100 nM. Under the optimized conditions, the fluorescence intensity of the solution of **RS2** was nearly proportional to the amount of Hg^{2+} added (0−2 ppb, R^2 = 0.998), establishing that **RS2** was capable of distinguishing safe and toxic levels of

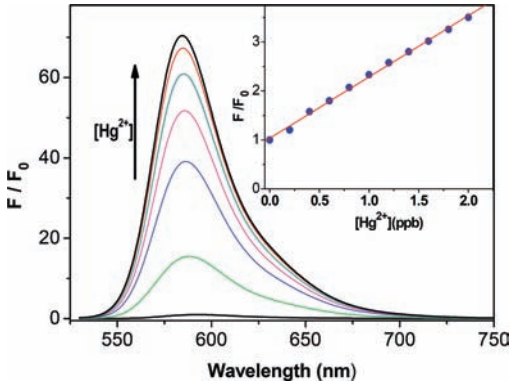

Figure 9. Fluorescence response of **RS2** (10 μM) upon addition of Hg^{2+} (0 to 0.2 mM) in an aqueous solution. Inset picture shows the fluorescence at 585 nm of compound **RS2** (0.1 μM) as a function of the mercury concentration (0.4−2 ppb). Excitation was at 510 nm. Spectra were recorded 4 min after adding Hg^{2+}.

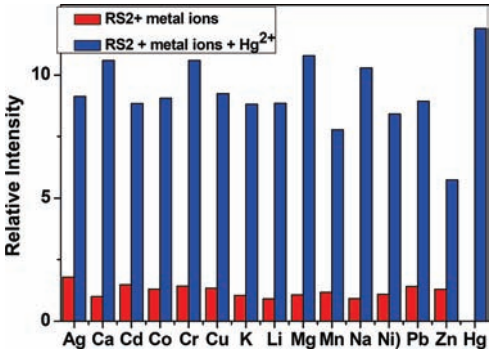

Figure 10. Fluorescence responses of **RS2** to various cations in aqueous solution ([**RS2**] = 10 μM; λ_{ex} = 510 nm). The red bars represent the emission intensities of **RS2** in the presence of 1.25 mM of Na^+, K^+, Ca^{2+}, and Mg^{2+} and 0.5 mM of the other cations of interest, respectively. The blue bars represent the change of the emission that occurs upon the subsequent addition of 0.1 mM of Hg^{2+} to the above solution. Spectra were recorded 4 min after mixing the different target ions.

inorganic mercury in drinking water according to the 2 ppb U.S. EPA standard[9] and 1 ppb China SA standard.[69] Alternatively, the spirolactam congener **RP1** (Scheme 1) could not be used to detect Hg^{2+} in pure water;[44] thus the incorporation of sulfur atom could improve the sensitivity for Hg^{2+} significantly. Despite that several small molecular chemosensors have the potential to detect Hg^{2+} in aqueous solutions at the parts per billion level,[10,11] the real-time detection of Hg^{2+} below 1 ppb with the fluorescent responses proportional to the amount of Hg^{2+} in natural water is still significant.

The fluorescence enhancement effects of various metal ions on **RS2** in aqueous solution were also investigated under excitation at 510 nm. As shown in Figure 10, no significant spectral changes of **RS2** occurred in the presence of alkali or alkaline-earth metals, such as Na^+, K^+, Mg^{2+}, Ca^{2+} and the first row transition metal Mn^{2+}, Fe^{2+}, Co^{2+}, Ni^{2+}, Cu^{2+}, respectively. The presence of 25 equiv excess of its group 12 congeners Zn^{2+} and Cd^{2+}, respectively, in addition to Pb^{2+} and Ag^+ did not induce any obvious fluorescence response. It was probably due to several combined influences cooperating to achieve the unique selectivity for the Hg^{2+} ion, such as the sulfur-affinity character of the Hg^{2+} ion, the suitable coordination geometry conformation of the Schiff-based chelating

(69) Standardization Administration of the People's Republic of China *Standard examination methods for drinking water - Metal parameters*, GB/T 5750.6-**2006**.

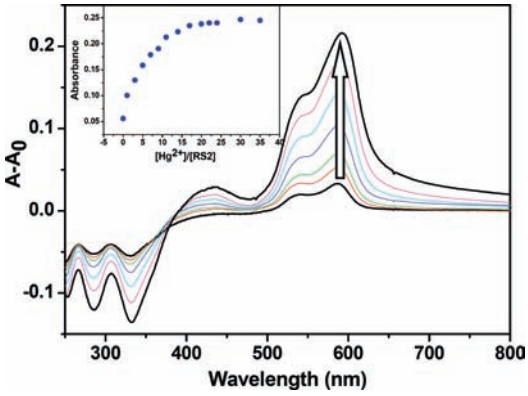

Figure 11. Different UV-vis spectra of **RS2** (50 μM) upon addition of Hg^{2+}. The inset picture shows the titration profile around 590 nm. Spectra were recorded 4 min after adding Hg^{2+}.

receptor.[45] The competition experiments revealed that the Hg-induced luminescence response were unaffected in the background of 25 equiv of environmentally relevant alkali or alkaline-earth metals, such as Na^+, K^+, Mg^{2+}, and Ca^{2+}. In addition, the first row transition metal ions, including Mn^{2+}, Co^{2+}, Ni^{2+}, Cu^{2+}, in addition to Pb^{2+} and Ag^+ had little interfere with the Hg^{2+}-induced fluorescence increase. However, the addition of Zn^{2+} compromised the Hg^{2+}-induced fluorescence enhancement of the **RS2**; it should be due to the coordination competing between Zn^{2+} and Hg^{2+}.

The absorption spectra of **RS2** in aqueous solution (50 μM) exhibited only a very weak band at 590 nm which was ascribed to the thiospirolactam form of probe **RS2**. Upon the addition of 10 equiv of Hg^{2+}, the absorption at 590 nm was significantly enhanced (log ε = 4.31; Figure 11), suggesting the formation of the ring-opened form of **RS2** upon Hg^{2+} binding. Like that in the related compound **RP1** (Scheme 1), the linear fitting of the titration curve assumed a 1:2 stoichiometry for the Hg^{2+}/**RS2** complexation species and yielded an association constant K_a of about 7.6×10^9 M^{-2}.

Electrospray ionization mass spectrometry (ESI-MS) spectra of a Hg/**RS2** solution revealed the presence of two main peaks. The base peak at m/z 662.08 corresponding to $[Hg(\mathbf{RS2})_2]^{2+}$ (m/z_{calcd} = 662.24) was clearly observed when 1.2 equiv of Hg^{2+} was added to **RS2**(50 μM) (Figure 12). The presence of a weak peak at m/z about 798.49 might be assigned to $[Hg(\mathbf{RS2})(OH)(H_2O)]^+$ (m/z_{calcd} = 798.24) complexation species.[70] Coordination of $[Hg(\mathbf{RS2})_2]^{2+}$ was proposed to involve the thioether S and the imino N atoms of both ligands, forming two stable 5-membered rings and delocalized xanthene moieties.

The selectivity of the UV-vis response of **RS2** to all the tested metal ions was also studied. While there were no significant absorption spectral changes of **RS2** that occurred in the presence of 50 equiv of Na^+, K^+, Mg^{2+}, Ca^{2+}, Zn^{2+}, Cd^{2+} and Pb^{2+}, respectively (Figure 13), the presence of 50 equiv of Mn^{2+}, Co^{2+}, and Ni^{2+} caused ignored absorption enhancement. Even, the addition of 50 equiv Ag^+ and Cu^{2+} could only cause the <15% absorbance enhancement compared to that of the addition of 10 equiv Hg^{2+}. The probe **RS2** showed good selectivity on both fluorescent and absorbance detection of Hg^{2+} in the presence of a high concentration of coexisting metal ions.

Structural and Spectroscopic Properties of RS3. Recently, we have also reported a new and practical multiresponsive chemosensor **RF1** (Scheme 1) by combining a ferrocene unit with a Rhodamine 6G block into one molecule via a carbohydrazone linkage which led to an excellent Hg^{2+}-specific responses in both electrochemical and optical detections.[45] It is believed that the incorporation of an electron-rich ferrocenyl group into the rhodamine-thiolactam system could enhance the coordination ability of the hydrazone nitrogen atom to Hg^{2+} ion. Meanwhile, the spatial effects of the uncoordinated ferrocenyl group are likely to affect the coordination ability of the sensor to the transition metal ions with constraint geometries and certain coordination numbers and would improve the selectivity of the sensor for detecting Hg^{2+} over transition metal ions.[45,71]

As shown in Figure 14, X-ray crystallography investigation exhibited the existence of a thiospirocyclic structure with the C_4S spiro ring in solid state. The C(8)−S(1) distance of 1.734(8) Å and the C(8)=N(1) of 1.280(8) Å indicated the existence of a C−S single bond and a C=N double bond of the thiolactam structure and the C(8)−N(1)−N(2)−C(9) torsion angle of 15° kept in the same range with **RS1** and **RS2**. The substance **RS3** could work well in water solution (1 μM), except the introduction of 0.5% (v/v) of DMF from the stock solution, within the relatively wide pH range (4.0 to 10.0), did not exhibit a significant emission band when excited at 500 nm.

The complexation of Hg^{2+} by **RS3** was investigated by means of fluorescence titration in aqueous solution (Figure 15). Upon the addition of Hg^{2+}, the emission band with the maximum emission at 550 nm appeared and developed. In the presence of 10 equiv of Hg^{2+}, the mixture showed an intense red fluorescence with a quantum yield of 0.61, and an approximate 125-fold enhancement in the fluorescence intensity at 550 nm, similar to the fluorescent behavior of **RF1**. This might simply be ascribed to the delocalized xanthene moiety of the rhodamine group. The introduction of a ferrocenyl group did not influence the typical emission of the rhodamine fluorophore, lending support to the rationality of our design strategy. The improved Benesi−Hildebrand analysis of the emission data gave a 1:1 stoichiometry for the complex [**RS3**-Hg], with an association constant (K_a) of 3.33×10^6 M^{-1} in aqueous medium, which is lager than that of **RF1**-Hg complexation.

Generally, the application of small molecular fluorescence detectors for Hg^{2+} in natural water samples

(70) Of course, it could not be proven beyond a shadow of a doubt that a small part of $[Hg(\mathbf{RS2})(OH)(H_2O)]^+$ species was present in ESI-MS experimental conditions. However, both the lower intensity of the +1 charge species compared to the +2 charge $[Hg(\mathbf{RS2})_2]^{2+}$ species and the excellent fitting of the linear with the titration curve supported that the 1:2 stoichiometric Hg^{2+}/**RS2** complexation species $[Hg(\mathbf{RS2})_2]^{2+}$ was the major and basilica species in titration solution.

(71) Caballero, A.; Martínez-Máñez, R.; Lloveras, V.; Ratera, I.; Vidal-Gancedo, J.; Wurst, K.; Tarraga, A.; Molina, P.; Veciana, J. *J. Am. Chem. Soc.* **2005**, *127*, 15666–15667.

(72) The imperfect isobestic points of the titration spectra below 325 nm might come from the absorbance of the small amount DMF about 0.5% (v/v) of the stock solution, especially for the different absorption spectra, in quite small concentration of **RS3** (10 μM).

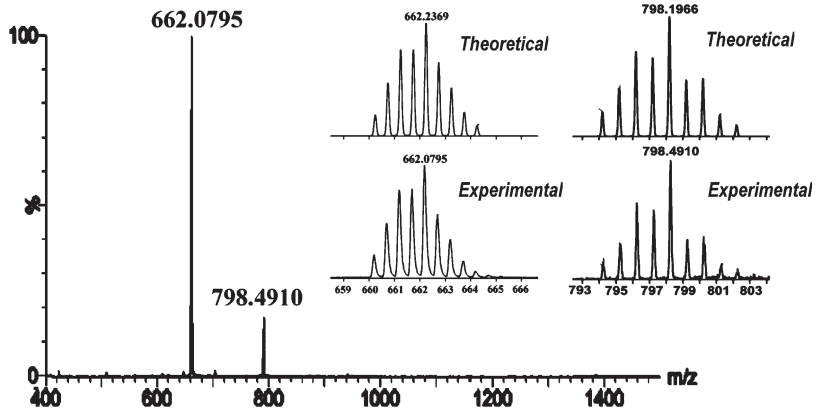

Figure 12. ESI-MS of the titration solution of **RS2** (50 μM) upon the addition of Hg^{2+} (60 μM). The inset exhibits the calculated (top picture) and observed (bottom picture) isotopic patterns for the $[Hg(\mathbf{RS2})_2]^{2+}$ (left)and $[Hg(\mathbf{RS2})(H_2O)(OH)]^{+}$ (right) cations.

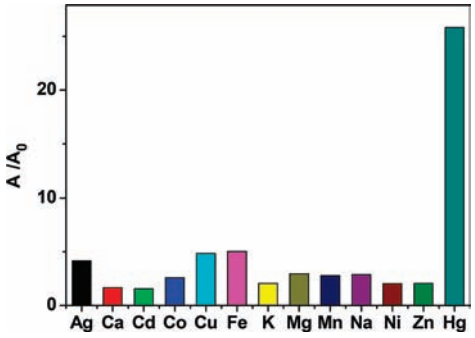

Figure 13. Absorbances at 590 nm of **RS2** (50 μM) in an aqueous solutions in the presence of 5 equiv of different metal ions.

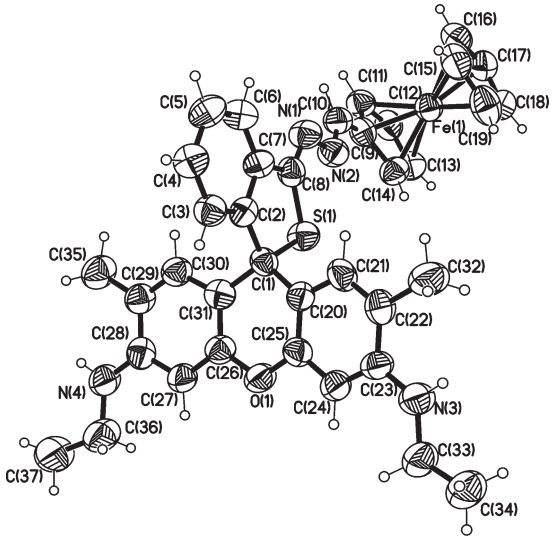

Figure 14. Molecular structure of **RS3** showing the thiospirolactam tautomer. Selected bond (Å) distances and angles (deg): C(8)−S(1) 1.734(8), C(1)−S(1) 1.883(7), C(8)−N(1) 1.280(8), N(1)−N(2) 1.408(8), N(2)−C(9) 1.277(8); C(8)−S(1)−C(1) 94.8(4), S(1)−C(8)−N(1) 128.1(6), C(8)−N(1)−N(2) 107.8.1(7), N(1)−N(2)−C(9) 112.5(7), N(2)−C(9)−C(10) 122.7(8).

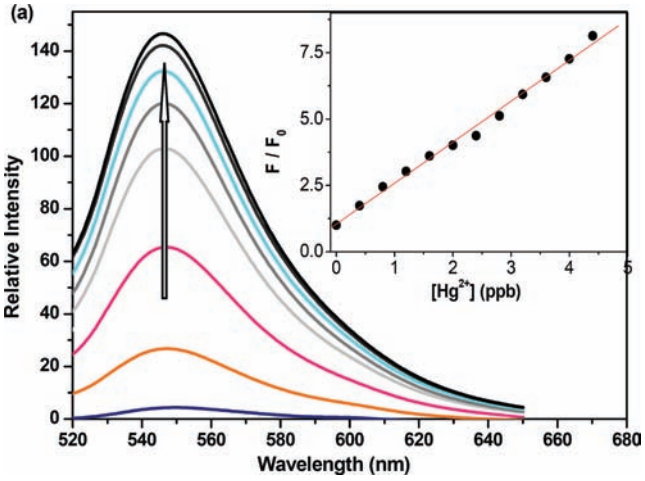

Figure 15. Fluorescence response of **RS3** (10 μM) upon addition of Hg^{2+} (0 to 0.2 mM) in an aqueous solution. Inset picture shows the fluorescence at 550 nm of compound **RS3 (0.1**μM) as a function of the mercury concentration (0−4 ppb). Excitation was at 500 nm. Spectra were recorded 4 min after adding Hg^{2+}.

presents a unique set of challenges, which requires detailed studies of sensor performance in the environmental milieu and method/device design. Owing to its optical Hg^{2+}-induced brightness, **RS3** is sensitive enough to detect environmentally relevant concentrations of Hg^{2+} ions in natural water. Addition of 0.4 ppb of Hg^{2+} ion to an aqueous solution of **RS3** affords a three-quarters increase of emission intensity. The fluorescence profile of **RS3** (0.1 μM) upon the titration of Hg^{2+} shown in the inset in Figure 15 also demonstrates that the limit of detection for Hg^{2+} is at the parts per billion level. Under the experimental conditions, the fluorescence intensities of the solution of **RS3** are nearly proportional to the amount of Hg^{2+} (0.4−5 ppb, R^2 = 0.99), indicating that **RS3** is capable of distinguishing between the safe and toxic levels of inorganic mercury in drinking water.

To obtain an excellent chemosensor, high selectivity is a matter of necessity. In the present work, studies of selective coordination of cations of **RS3** by means of fluorescence spectroscopy were then extended to related heavy, transition, and main group metal ions. Only the addition of Hg^{2+} resulted in a prominent fluorescent change in fluorescence, whereas only very little variation occurred in the presence of millimolar levels of alkali or alkaline earth metals and first row transition metals, including Cu^{2+}, Pb^{2+}, and Ag^{+}. The competition experiments revealed that the Hg-induced luminescence response was unaffected in the background of the above-mentioned metal ions, indicating an excellent selectivity toward Hg^{2+} of **RS3** (Figure 16).

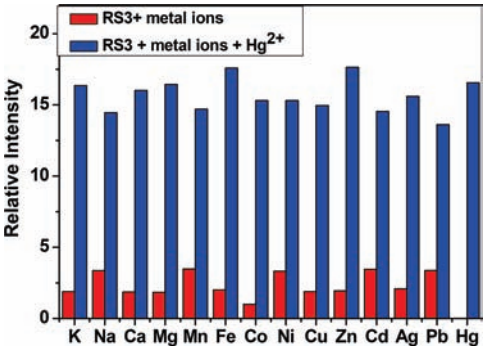

Figure 16. Fluorescence responses of **RS3** to various cations in an aqueous solution ([**RS3**] = 10 μM; λ_{ex} = 500 nm). The red bars represent the emission intensities of **RS3** in the presence of 1.25 mM of Na^+, K^+, Ca^{2+}, and Mg^{2+} and 0.5 mM of the other cations of interest, respectively. The blue bars represent the change of the emission that occurs upon the subsequent addition of 0.1 mM of Hg^{2+} to the above solution. Spectra were recorded 4 min after mixing the different target ions.

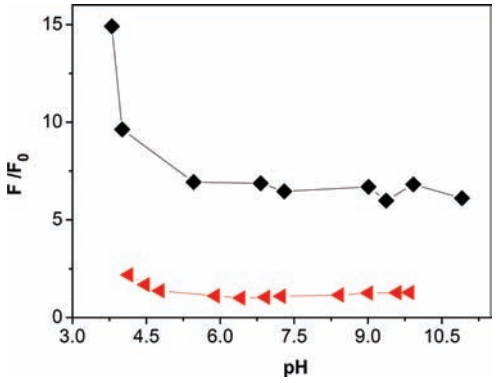

Figure 17. pH-dependent fluorescence responses of **RS3** (10 μM) (red triangle) and **RS3** (10 μM) plus Hg^{2+} (20 μM) (black rectangle) in aqueous solution. The luminescence intensities were recorded at 550 nm with the excitation wavelength of 500 nm.

The pH−control emission measurements revealed that **RS3** could respond to Hg^{2+} in the pH range from 4.5 to 10.0 with the fluorescent intensity varying less than 10%, while the luminescence of the free **RS3** can be negligible. When the pH value was lower than 4.0, the fluorescence enhancement occurred also upon the coordination of Hg^{2+}, but the luminescence intensity of the free **RS3** increased slowly with the decreasing pH values. It could be seen that the **RS3** facilitates quantification of the concentration of Hg^{2+} in aqueous solution in a wide pH range (Figure 17).

The absorption spectra of Hg^{2+}-free **RS3** (10 μM) were investigated in aqueous solution. The UV selectivity of **RS3** have been improved significantly relative to **RS1** and **RF1** (scheme 1), even the addition of Ag^+ and Cu^{2+} into the solution under the same conditions, could not induce any obvious enhancement of absorbance at about 500 nm (Figure 18). The higher selectivity of **RS3** over **RS2** on the UV spectral response for Hg^{2+} indicated that the spatial effect of a large rhodamine unit and the ferrocene groups probably affected the binding ability to metal cations, especially for the transition metals with constraint geometries and certain coordination numbers. Consequently, the lack of additional binding sites of **RS3** would make the probe show no or little coordination to any other metal ions, but allow the most preferred mercuric ion to bind.

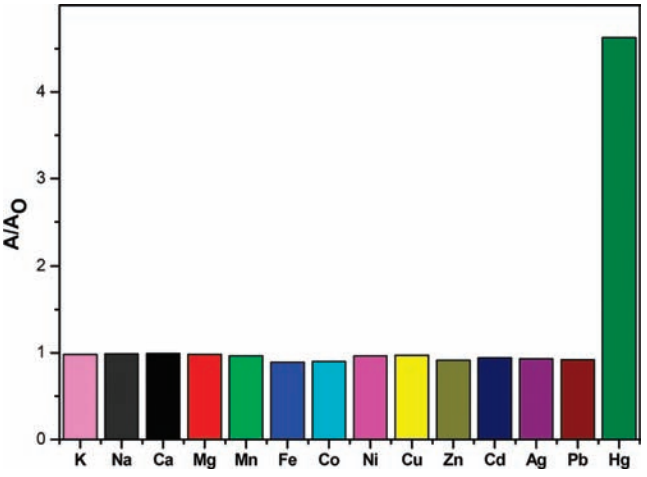

Figure 18. Absorption at 500 nm of **RS3** (50 μM) in an aqueous solution in the presence of 5 equiv of different metal ions. Spectra were recorded 4 min after adding Hg^{2+}.

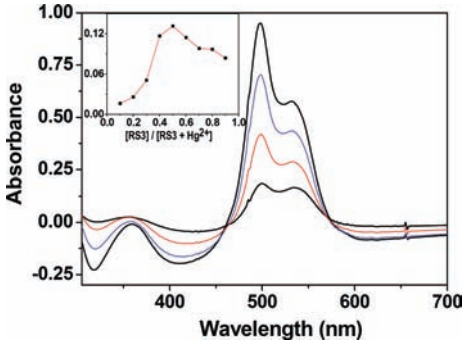

Figure 19. Different UV−vis spectra of **RS3** (10 μM) upon addition of Hg^{2+}. The inset picture shows the Job's plot at about the absorbance 500 nm.[72] Spectra were recorded 4 min after adding Hg^{2+}.

The addition of 5 equiv of Hg^{2+} caused the new peak at about 500 nm to be significantly enhanced (log ε = 4.38; Figure 19). Accordingly, the titration solution exhibited an obvious and characteristic color change from colorless to pink. It suggested that **RS3** could be used for a "naked-eye" detection of Hg^{2+} ions in aqueous environment. The 1:1 stoichiometry for complex [**RS3**-Hg^{2+}] was also indicated by a Job's plot evaluated from the absorption spectra.

ESI-MS spectra of a Hg/**RS3** solution revealed the presence of two main peaks (Figure 20). The two distinct peaks with m/z = 841.09 and 877.06 when 1.2 equiv of Hg^{2+} were added to **RS3** (10 μM), corresponding to the species [**RS3**-Hg-(H)]$^+$ (m/z_{calcd} = 841.16) and [**RS3**-Hg-(H_2O)(OH)]$^+$ (m/z_{calcd} = 877.13), respectively, in referring to the exact comparison of the peaks with the simulation on the basis of natural isotopic abundances. The very weak peak at about 741.17 was assigned to the species [$(\mathbf{RS3})_2$-Hg]$^{2+}$ (m/z_{calcd} = 740.92), indicating the presence of trace amount of [$(\mathbf{RS3})_2$-Hg]$^{2+}$ species in the solution.

Electrochemical methods, in particular, are extremely attractive because the signals can be easily read out *on-site* from a practical standpoint.[73−75] Since the ferrocenyl

(73) Tchinda, A. J.; Ngameni, E.; Walcarius, A. *Sens. Actuators, B* **2007**, *121*, 113–123.
(74) Singh, P. R.; Contractor, A. Q. *Int. J. Environ. Anal. Chem.* **2005**, *85*, 831–835.
(75) Crouse, M. M.; Miller, A. E.; Crouse, D. T.; Ikram, A. A. *J. Electrochem. Soc.* **2005**, *152*, D167–D172.

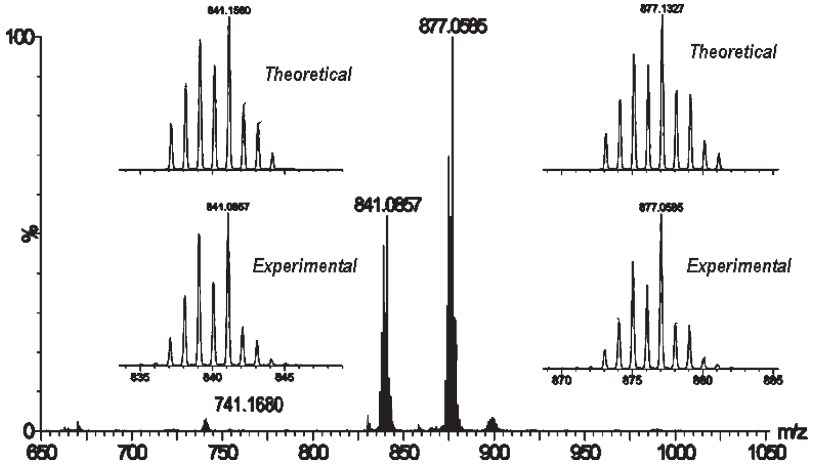

Figure 20. ESI-MS of the titration solution of **RS3** (50 μM) upon the addition of Hg^{2+} (60 μM). The insets exhibit the calculated (top picture) and observed (bottom picture) isotopic patterns for the [**RS3**-Hg-(H)]$^+$ (left) and [**RS3**-Hg(H_2O)(OH)]$^+$ (right) cations, respectively.

group is coplanar with the phenyl ring of the rhodamine moiety, the electronic density within the ferrocene group is influenced by the electron proportion of the optical sensitive rhodamine moiety induced by Hg^{2+}-binding.[17,45] As expected, **RS3** exhibited obvious change in its reversible ferrocene/ferricinum redox cycles.[76−80] Cyclic voltammetry (CV) of the substance **RS3** (0.5 mM) in mixed solution (CH_3CN: H_2O = 7: 3) exhibited a reversible one electron redox reaction around 100 mV (vs Fc^+/Fc). Whereas no perturbation of the CV and differential pulse voltammetry (DPV) was observed upon addition of alkali and earth alkali metal ions, or Ni^{2+}, Zn^{2+}, and Cd^{2+}. The addition of 1 equiv of Hg^{2+} induced a significant modification with an anodic shift ($\Delta E_{1/2}$) of 100 mV (Figure 21), which was larger than the 50 mV of **RF1**. The DPV also exhibited an anodic shift ($\Delta E_{1/2}$ = 140 mV) and a new peak at 0.187 V (vs Fc^+/Fc) upon the complexation of Hg^{2+} in aqueous CH_3CN solution. The sensitivity of the **RS3** was improved in both spectral and electrochemical detection compared with **RF1**, which suggested the stronger affinity of **RS3** toward Hg^{2+} by the replacement of the O atom with S atom. The reversibility of the ferrocene/ferrocenium redox couple of **RS3** in the presence of 0.25 equiv Hg^{2+} was confirmed by the linear relation between peak currents and the square root of the scan rates (Figure 22), the small difference between anodic and cathodic peak currents, as well as the small peak-to-peak potential separations.

Several thiophilic mercury-selective chemosensors or chemodosimeters have been developed, most of them exploited an irreversible mercury-promoted desulfurization reaction.[28−30] For a chemical sensor to be widely employed in the detection of specific analytes, the reversibility is an important aspect. Addition of metal cation leads to a spirocycle opening via coordination or

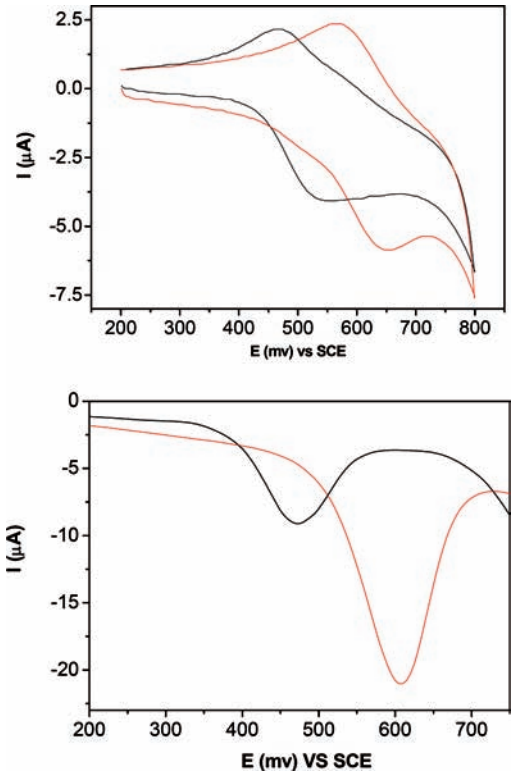

Figure 21. (top) CV in CH_3CN/H_2O (7/3, 0.5 mM) of free **RS3** (black) and after formation of RS1-Hg^{2+} (red) with [(n-Bu)$_4$N]ClO_4 as supporting electrolyte. (bottom) DPV in CH_3CN/H_2O (7/3, 0.5 mM) of free **RS3** (black) and after addition of 1.0 equiv (red) of Hg^{2+} respectively with [(n-Bu)$_4$N]ClO_4 as supporting electrolyte.

irreversible chemical reaction, resulting in an appearance of pink color and orange fluorescence. The addition of an aqueous solution of Na_2S (0.1M) to the solutions of **RS**s−Hg^{2+} species diminishes the fluorescence significantly down the initial value of free probes themselves, respectively (Figure 23). This is not surprising since S^{2-} has a reported K_d value of 10^{-50} M^2 for Hg^{2+} at a standard condition in the form of $[HgS_2]^{2-}$.[81,82] Thus, the response

(76) Beer, P. D. *Acc. Chem. Res.* **1998**, *31*, 71–80.
(77) Ornelas, C.; Aranzaes, J. R.; Cloutet, E.; Alves, S.; Astruc, D. *Angew. Chem., Int. Ed.* **2007**, *46*, 872–877.
(78) Otón, F.; Tárraga, A.; Tarraga, A.; De Arellano, C. R.; Molina, P. *Chem.—Eur. J.* **2007**, *13*, 5742–5752.
(79) Zapata, F.; Caballero, A.; Espinosa, A.; Tarraga, A.; Molina, P. *Org. Lett.* **2007**, *9*, 2385–2388.
(80) Zhou, Z.; Yu, M.; Yang, H.; Huang, K.; Li, F.; Yi, T.; Huang, C. *Chem. Commun.* **2008**, 3387–3389.
(81) Findlay, D. M.; McLean, R. A. N. *Environ. Sci. Technol.* **1981**, *15*, 1388–1390.
(82) Armstrong, R. D.; Porter, D. F.; Thirsk, H. R. *J. Phys. Chem.* **1968**, *72*, 2300–2306.

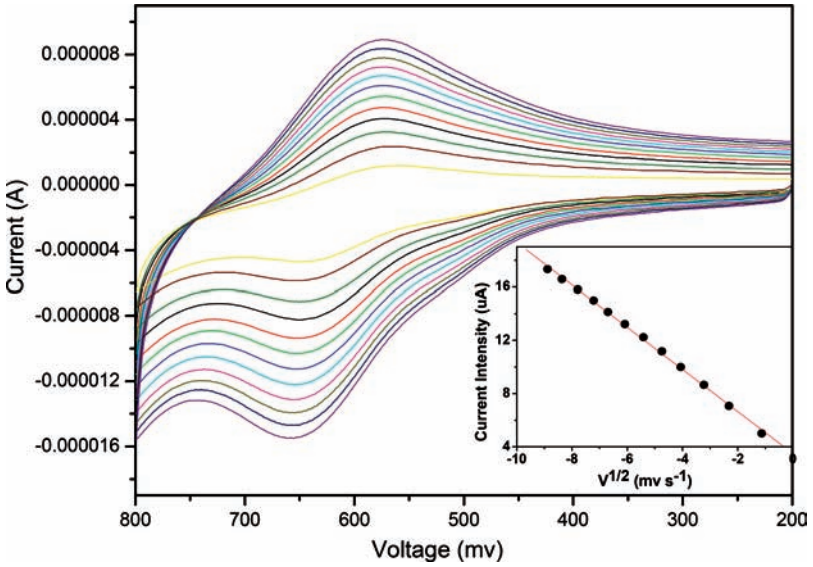

Figure 22. Family of CV curves of the **RS3-Hg**$^{2+}$ complexation species showing the changes of current with the scan rate, [(*n*-Bu)$_4$N]ClO$_4$ (100 mM) as supporting electrolyte. The inset shows plots of anodic peak currents versus the square root of the scan rates, $V^{1/2}$.

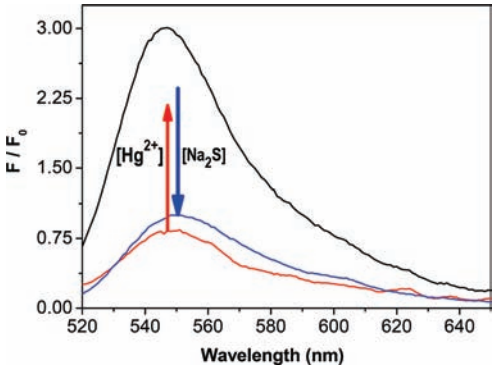

Figure 23. Reversibility of Hg^{2+} coordination to **RS3** by Na_2S. Red line, free **RS3** (1 μM), black line, **RS3** + 1 equiv of Hg^{2+}. Blue line: **RS3** + 1 equiv of Hg^{2+} + 1.95 mL of Na_2S (0.5 mM).

of **RS**s to Hg^{2+} is reversible rather than a cation-catalyzed reaction.

Conclusion

In a summary, we have reported new rhodamine thiospirolactons for the selective detection of Hg^{2+} in aqueous solutions. **RS**s can selectively bind Hg^{2+} over other Group 12 metals, most divalent first-row transition metals and millimolar concentrations of various alkali and alkaline earth metals. The parts per billion level fluorescent detection limit suggests the possibility of practical applications in toxicology and environmental sciences. X-ray crystal structure analyses reveal the thioethers of the spirolacton, which ensure the opening of the spirolactam ring directly through the metal-binding of the sulfur atom. The poorer coordination affinity of the thioethers toward the first-row transition metal ions compared to the thioamides suggests the possible selectivity for Hg^{2+} over other interference metal ions, especially the sulfurphilic metal ions. The high sensitivity and the selectivity for Hg^{2+} ion of **RS**s is in part because of several cooperative origins: the suitable coordination conformation of the Schiff-based receptor, the large radius of the Hg^{2+} ion, the Sulfur-affinity character of the Hg^{2+} ion, and the electronic or spatial effects of the additional aromatic or ferrocenyl group. Our future research efforts will concentrate on the development of new testing methods, such as immobilization of the sensors on a membrane, test paper, or mesoporous materials,[83] to improve the recognition ability of **RS**s and their derivatives toward different ions in the practical environment and media.

Acknowledgment. This work is supported by the National Natural Science Foundation and the Start-Up Fundation of Dalian University of Technology.

Supporting Information Available: X-ray structural data of **RS**s in CIF format. This material is available free of charge via the Internet at http://pubs.acs.org.

(83) Gao, L.; Wang, Y.; Wang, J. Q.; Huang, L.; Shi, L. Y.; Fan, X. X.; Zou, Z. G.; Yu, T.; Zhu, M.; Li, Z. S. *Inorg. Chem.* **2006**, *45*, 6844–6850.